

ChemComm

Accepted Manuscript



This is an *Accepted Manuscript*, which has been through the Royal Society of Chemistry peer review process and has been accepted for publication.

Accepted Manuscripts are published online shortly after acceptance, before technical editing, formatting and proof reading. Using this free service, authors can make their results available to the community, in citable form, before we publish the edited article. We will replace this *Accepted Manuscript* with the edited and formatted *Advance Article* as soon as it is available.

You can find more information about *Accepted Manuscripts* in the [Information for Authors](#).

Please note that technical editing may introduce minor changes to the text and/or graphics, which may alter content. The journal's standard [Terms & Conditions](#) and the [Ethical guidelines](#) still apply. In no event shall the Royal Society of Chemistry be held responsible for any errors or omissions in this *Accepted Manuscript* or any consequences arising from the use of any information it contains.

COMMUNICATION

Porous Graphene-based Material as an Efficient Metal Free Catalyst for the Oxidative Dehydrogenation of Ethylbenzene to Styrene †

Cite this: DOI: 10.1039/x0xx00000x

Received 00th January 2012,
Accepted 00th January 2012

Jiangyong Diao,^{a,b} Hongyang Liu,^a Jia Wang,^{a,b} Zhenbao Feng,^a Tong Chen,^c Changxi Miao,^c Weimin Yang^{*c} and Dang Sheng Su^{*a}

DOI: 10.1039/x0xx00000x

www.rsc.org/

Reduced porous graphene oxide as a metal free catalyst was selected for the oxidative dehydrogenation of ethylbenzene to styrene. It showed the best catalytic performance compared with other carbon materials (routinely reduced graphene oxide, graphite powder and oxidized carbon nanotubes) and commercial iron oxide.

Styrene (ST) is an important industrial monomer which is mainly produced by direct dehydrogenation (DH) of ethylbenzene (EB). Generally, this DH reaction is catalyzed by potassium-promoted iron oxide catalyst under high temperature and excess steam.¹ The overheated steam is used to transfer heat and remove carbonaceous species which are produced during the DH reaction and can cause the loss of reaction activity. Therefore, this mode of styrene production is energy intensive and environment unfriendly. Recently, some alternative routes have been put forward, such as side-chain alkylation of toluene with methanol² and oxidative dehydrogenation (ODH) with O₂, CO₂ or N₂O.³ However, the present techniques still employ unsustainable metal/metal oxide compounds or suffer a low activity. Hence, alternative catalysts need to be explored to overcome these aforesaid problems.

Nanocarbon materials with unique properties have been proved to be efficient catalysts for the DH and ODH of hydrocarbons.⁴ Many kinds of nanocarbons such as multiwalled carbon nanotubes (MWCNTs), mesoporous carbon, nanodiamond and onion-like carbon have been investigated for DH/ODH of ethylbenzene to styrene.⁵ Graphene as a monolayer planar sheet composed of sp²-bonded carbon atoms possesses unique electrical, thermal and optical properties,⁶ and it has shown excellent performance in supercapacitors, fuel cells and lithium ion batteries.⁷ Recently, graphene based-materials were widely investigated in liquid phase catalytic fields and showed potential applications.⁸ However, only a few studies in gas-phase catalytic reactions have been reported.⁹

Herein, we systematically investigated the catalytic performance of the reduced porous graphene oxide (rPGO) in the ODH of EB to ST.

Compared with the routinely reduced graphene oxide (rGO), the oxidized carbon nanotubes (oCNT), the graphite powder (GP) and the commercial iron oxide catalyst, the rPGO with high specific surface area (2613 m²/g), high porosity and abundant oxygen functional groups exhibits the best catalytic performance with a 65 % EB conversion and a 93 % ST selectivity. Meanwhile, the long term catalytic stability indicates the potential application of the rPGO catalyst in the industrial styrene production.

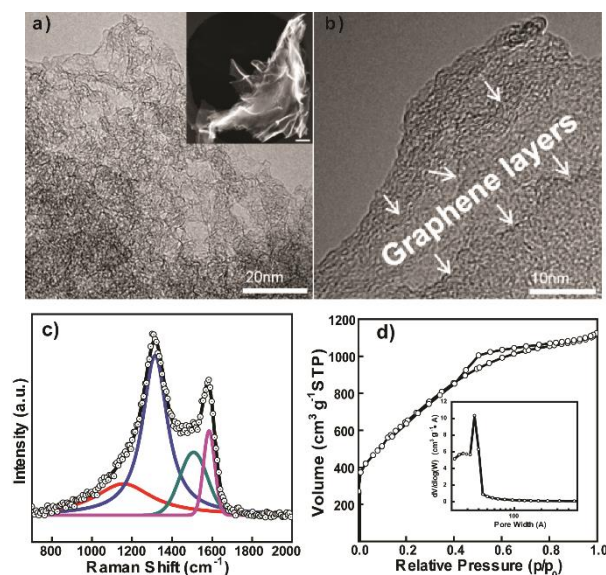


Fig. 1 a), b): TEM images of the rPGO with different magnifications. The inset in Fig. 1a is the high resolution SEM image of the rPGO (scale bar: 250 nm). c) Raman spectrum and peak fitting of the rPGO; d) N₂ adsorption-desorption isotherms with the pore size distribution (inset) of the rPGO.

The detailed synthesis process of the rPGO can be found in the ESI and the other carbon materials such as the rGO, GP and oCNT are employed for the controlled experiments. A typical SEM image (the

inset in Fig. 1a) shows that the obtained rPGO catalyst is highly folded and self-assembled to a three dimensional morphology, and the curved graphene sheets of the rPGO are transparent to the electron beam. Besides, the multilayer, wrinkled and curved microstructure of the rPGO is also confirmed by TEM images (Fig. 1a & 1b), which is different from the rGO, GP and oCNT as shown in Fig. S1. In addition, from a typical high resolution TEM image, a few irregularly stacked layers can be clearly seen at the edge as marked in Fig. 1b.

Raman spectroscopy is an effective method to characterize the structure and defects of carbon materials.¹⁰ Generally, the D, D3, D4 peak at about 1350 cm^{-1} , 1500 cm^{-1} , 1200 cm^{-1} represent the disordered graphitic lattice (graphene layer edges), amorphous carbon, and disordered graphitic lattice (polyenes, ionic impurities) of carbon materials respectively, while the G peak at about 1580 cm^{-1} represents the ideal graphitic lattice of carbon materials. The intensity ratio of D peak and G peak (I_D/I_G) is usually an estimate of the disorder degree of carbon materials. From the Raman spectrum of the rPGO as displayed in Fig. 1c, the D and G peak could be obviously observed, indicating that the basic graphitic structure was maintained after the activation process. Meanwhile, the broad and strong D peak suggests that there exists lots of edge structure in the rPGO sample. The value of I_D/I_G calculated from the corresponding area of peak fitting is as high as 6.2, revealing that the rPGO is highly defective. The detailed structure of the rPGO is further confirmed by XRD analysis. The XRD results in Fig. S2 demonstrate that the rPGO has a similar graphitic structure with the natural graphite. However, the dominating graphite peak (002, $2\theta = 26.4^\circ$) intensity of the rPGO is drastically decreased and the peak width is broadened. Compared with the natural graphite, the high ratio of I_D/I_G , the low and wide (002) peak could be mainly attributed to the presence of a high density of pores in the rPGO,⁷ which is in well agreement with the TEM results.

N_2 adsorption-desorption isotherms of the rPGO show type-IV curves, with an obvious condensation step at $P/P_0 = 0.4-0.8$, suggesting a porous structure which may contain split and tubular pore geometry (Fig. 1d),¹¹ and the isotherms of the rGO is exhibited in Fig. S3 as a comparison. The specific surface area of the rPGO is about 2613 m^2/g calculated according to Brunauer-Emmett-Teller (BET) method, which is obviously larger than that of the rGO (127 m^2/g). The cumulative pore volume and average pore width calculated from the desorption branch according to Barrett-Joyner-Halenda (BJH) model is about 2.3 cm^3/g and 3.2 nm, respectively. The pore size distribution curve (the inset in Fig. 1d) displays that the rPGO has well-defined micro- and mesopores. These pores mainly originated from the etching process by KOH during high temperature reduction,^{7, 12} and could explain the high disorder degree and plenty of graphene layer edges which are revealed by the Raman results. Moreover, the widespread pores may not only provide plenty of unpaired electrons which induce the occurrence and proceeding of a catalytic reaction, but also act as the transport pathways for the reaction species.^{9, 13} In short, the huge surface area and unique texture of the rPGO provide an exciting possibility in the oxidative dehydrogenation of EB to ST.

As to ODH reactions, the oxidation resistance ability of the nanocarbon catalysts is very important for their practical applications. The thermal stability behavior of the rPGO was monitored by Thermogravimetry-Mass Spectrometry (TG-MS) in excess oxygen (5% O_2/Ar) in this work. The result is shown in Fig. S4. From the TG-MS curves, we can see that the rPGO exhibits well stability below 500 $^\circ\text{C}$, and CO_2 signal corresponding to the combustion of the rPGO is just

detected above 500 $^\circ\text{C}$. In addition, the optimization experiments of reaction condition show a steady conversion below 425 $^\circ\text{C}$ and a favourable selectivity at $\text{O}_2/\text{EB} = 1$ (Fig. S5 & Fig. S6).

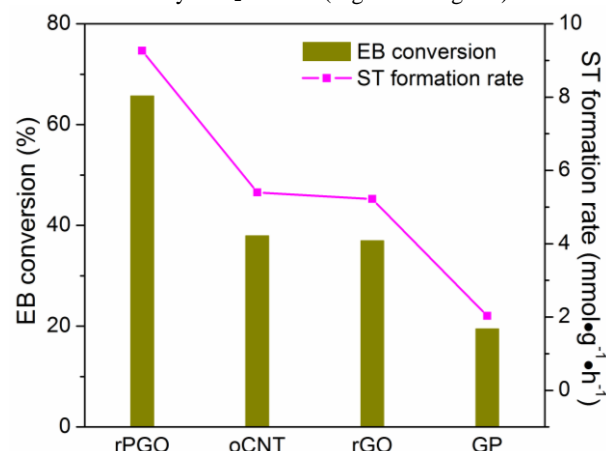


Fig. 2 Catalytic performance of different carbon materials on ODH of EB, data from 30 h on stream. Reaction condition: 50 mg catalyst, 3 % EB with He balance, $\text{O}_2/\text{EB} = 1$, total flow rate = 10 ml/min, $T = 400^\circ\text{C}$.

Fig. 2 represents the catalytic performance of different carbon materials (rPGO, oCNT, rGO, GP) on ODH of EB at 400 $^\circ\text{C}$. Among all the carbon materials, the rPGO catalyst exhibits the highest EB conversion (65 %) and ST formation rate ($9.27 \text{ mmol}\cdot\text{g}^{-1}\cdot\text{h}^{-1}$), while those of the other three catalysts are all less than 40 % and 6 $\text{mmol}\cdot\text{g}^{-1}\cdot\text{h}^{-1}$ after 30 h on stream. As to the styrene selectivity, it is higher than 90 % over all the tested catalysts (Fig. S7). GP has the highest ST selectivity (97%), but its conversion is only around 20 % due to its low oxygen content and stacked structure, which is similar with the reported results.⁵ Besides, the commercial iron oxide catalyst was also tested as a controlled catalyst (Fig. S8), which presented quite low activity (a 3 % EB conversion and a 20 % ST selectivity). Long term stability of the rPGO was also conducted at 400 $^\circ\text{C}$ (Fig. S9). After a 30 h induction period, the EB conversion over the rPGO reaches a steady platform, the highest value is 54 % and it still maintains at 50 % after 80 h reaction, while the ST selectivity is stabilized at around 95 % during the whole process. The structural and catalytic robustness of the rPGO could be further confirmed by the characterizations of the used catalyst (Fig. S10), which reveal that the rPGO has well combustion resistance ability under the given reaction condition. In addition, compared with the reported nanocarbon materials (table S1), the present rPGO catalyst exhibits the best catalytic performance in the ODH of EB to ST.

In order to further understand the high catalytic performance of the ODH reaction over the rPGO catalyst, XPS is employed to analyze its surface composition. The C1s spectrum of the rPGO shows a clear shoulder peak at 288.7 eV (Fig. 3a), which is said to be carbonyl groups,⁹ and this can be further confirmed by peak fitting of O1s spectrum (Fig. 3b). The deconvolution of the O1s spectrum reveals three different chemical environments of O, which could be assigned to phenol groups (C-OH, $\sim 533.7 \text{ eV}$), the sum of carboxylic acid, anhydride, lactone and ester groups (O=C-O, $\sim 532.5 \text{ eV}$), and ketonic carbonyl group (C=O, $\sim 531.6 \text{ eV}$), respectively.¹⁴ The total surface oxygen atomic concentration in the rPGO is estimated from XPS spectrum to be 15.3 at% and the corresponding unsaturated C=O ratio is 40.8 %. The high oxygen content of the rPGO is probably due to its

ultrahigh surface area and high porosity. Generally, the basic sites have been demonstrated as active sites during the dehydrogenation reaction of hydrocarbons.^{14, 15} The rPGO catalyst with the highest reaction rate has the highest carbonyl concentration (table S2), corresponding to the fact that nucleophilic ketonic carbonyl groups are the active sites in the ODH reaction.¹⁶ Meanwhile, the oxygen molecules in the inlet gas can be easily absorbed and activated by the electron-rich pores distributed on the defective graphene layers, resulting in the formation of new oxygen functional groups such as ketone and quinone under reaction conditions as revealed by the used rPGO in table S2.¹⁷ These newly formed ketonic carbonyl groups also contribute to the catalytic activity of the rPGO. And the high porosity and novel pore structure of the rPGO can facilitate the mass and heat transfer of ODH reaction,^{12, 18} which restrains the generation of byproducts and leads to a high ST selectivity.

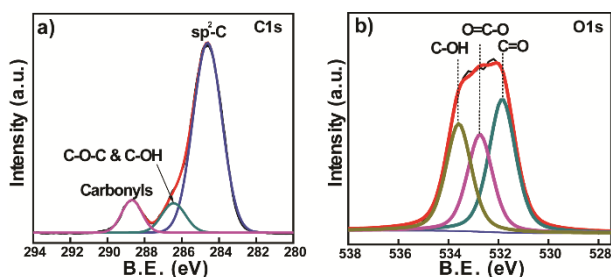


Fig. 3 C1s and O1s peak fitting curves of the rPGO.

In summary, the reduced porous graphene oxide was first used as a metal free catalyst for the oxidative dehydrogenation of ethylbenzene. The reduced porous graphene oxide showed the best catalytic performance (a 65 % EB conversion and a 93 % ST selectivity) compared with the other carbon materials and the commercial iron oxide catalyst. The special structure of the rPGO provides more anchor sites for oxygen functional groups on the defects, and the unpaired electrons at the edges of defects can attract and promote the activation of oxygen molecules in oxidizing atmosphere. The ultrahigh surface area and unique structure of the rPGO facilitate the adsorption-desorption process of reaction species, which avoids the deep oxidation of ST and the generation of byproducts, thus leading to a high styrene selectivity under a high EB conversion. The stable long term catalytic performance of the rPGO in the ODH reaction of ethylbenzene to styrene indicates its potential application as an industrial catalyst.

We would like to acknowledge the financial support by the National Natural Science Foundation of China (No. 21203214, 21133010, 21261160487, 51221264), the National Basic Research Program (973 Program, No. 2011CBA00504), the Sinopec China and the Strategic Priority Research Program of the Chinese Academy of Sciences, Grant No. XDA09030103.

Notes and references

^a Shenyang National Laboratory for Materials Science, Institute of Metal Research, Chinese Academy of Sciences, Shenyang 110016, China. E-mail: dssu@imr.ac.cn; Fax: +86 2483970019; Tel: +86 2423971577

^b University of Chinese Academy of Sciences, Beijing 100049, China.

^c Sinopec Shanghai Research Institute of Petrochemical Technology, 1658 Pudong Beilu, Shanghai, China. E-mail: yangwm.sshy@sinopec.com; Fax: +862168462283; Tel: +862168462824.

† Electronic Supplementary Information (ESI) available: the detailed production process of the rPGO, TEM images, XRD spectra, TG-MS results, activity tests at different reaction conditions, characterizations of the used rPGO and XPS analysis, see DOI: 10.1039/c000000x/

- (a) E. H. Lee, *Cat. Rev.*, 1974, **8**, 285; (b) M. Muhler, J. Schütze, M. Wesemann, T. Rayment, A. Dent, R. Schlögl and G. Ertl, *J. Catal.*, 1990, **126**, 339.
- J. M. Serra, A. Corma, D. Farrusseng, L. Baumes, C. Mirodatos, C. Flego and C. Perego, *Catal. Today*, 2003, **81**, 425.
- (a) M. F. R. Pereira, J. J. M. Órfão and J. L. Figueiredo, *Appl. Catal. A*, 1999, **184**, 153; (b) A. J. R. Castro, J. M. Soares, J. M. Filho, A. C. Oliveira, A. Campos and E. R. C. Milet, *Fuel*, 2013, **108**, 740; (c) N. R. Shiju, M. Anilkumar, S. P. Gokhale, B. S. Rao and C. V. V. Satyanarayana, *Catal. Sci. Technol.*, 2011, **1**, 1262.
- D. S. Su, S. Perathoner and G. Centi, *Chem. Rev.*, 2013, **113**, 5782.
- (a) D. S. Su, N. Maksimova, J. J. Delgado, N. Keller, G. Mestl, M. J. Ledoux and R. Schlögl, *Catal. Today*, 2005, **102–103**, 110; (b) J. Zhang, D. S. Su, R. Blume, R. Schlögl, R. Wang, X. Yang and A. Gajović, *Angew. Chem. Int. Ed.*, 2010, **49**, 8640; (c) H. Liu, J. Diao, Q. Wang, S. Gu, T. Chen, C. Miao, W. Yang and D. S. Su, *Chem. Commun.*, 2014, **50**, 7810.
- (a) K. S. Novoselov, A. K. Geim, S. V. Morozov, D. Jiang, Y. Zhang, S. V. Dubonos, I. V. Grigorieva and A. A. Firsov, *Science*, 2004, **306**, 666; (b) A. K. Geim and K. S. Novoselov, *Nat Mater*, 2007, **6**, 183.
- (a) Y. Zhu, S. Murali, M. D. Stoller, K. J. Ganesh, W. Cai, P. J. Ferreira, A. Pirkle, R. M. Wallace, K. A. Cyhosh, M. Thommes, D. Su, E. A. Stach and R. S. Ruoff, *Science*, 2011, **332**, 1537; (b) J. Hou, Y. Shao, M. W. Ellis, R. B. Moore and B. Yi, *Phys. Chem. Chem. Phys.*, 2011, **13**, 15384.
- (a) B. F. Machado and P. Serp, *Catal. Sci. Technol.*, 2012, **2**, 54; (b) S. Navalon, A. Dhakshinamoorthy, M. Alvaro and H. Garcia, *Chem. Rev.*, 2014, **114**, 6179.
- (a) C. Su, M. Acik, K. Takai, J. Lu, S.-j. Hao, Y. Zheng, P. Wu, Q. Bao, T. Enoki, Y. J. Chabal and K. Ping Loh, *Nat. Commun.*, 2012, **3**, 1298; (b) G. K. P. Dathar, Y.-T. Tsai, K. Gierszal, Y. Xu, C. Liang, A. J. Rondinone, S. H. Overbury and V. Schwartz, *ChemSusChem*, 2014, **7**, 483.
- (a) A. Sadezky, H. Muckenhuber, H. Grothe, R. Niessner and U. Pöschl, *Carbon*, 2005, **43**, 1731; (b) M. S. Dresselhaus, A. Jorio, M. Hofmann, G. Dresselhaus and R. Saito, *Nano Lett.*, 2010, **10**, 751.
- K. S. W. Sing, D. H. Everett, R. A. W. Haul, L. Moscou, R. A. Pierotti, J. Rouquerol and T. Siemieniowska, *Pure Appl. Chem.*, 1985, **57**, 603.
- M. Molina-Sabio and F. Rodriguez-Reinoso, *Colloid Surf. A Physicochem. Eng. Asp.*, 2004, **241**, 15.
- Y. Xu, Z. Lin, X. Zhong, X. Huang, N. O. Weiss, Y. Huang and X. Duan, *Nat. Commun.*, 2014, **5**, doi: 10.1038/ncomms5554
- W. Qi, W. Liu, B. Zhang, X. Gu, X. Guo and D. S. Su, *Angew. Chem. Int. Ed.*, 2013, **52**, 14224.
- D. S. Su, J. Zhang, B. Frank, A. Thomas, X. Wang, J. Paraknowitsch and R. Schlögl, *ChemSusChem*, 2010, **3**, 169.
- J. Zhang, D. Su, A. Zhang, D. Wang, R. Schlögl and C. Høbert, *Angew. Chem. Int. Ed.*, 2007, **46**, 7319
- (a) F. Atamny, J. Blöcker, A. Dübotzky, H. Kurt, O. Timpe, G. Loose, W. Mahdi and R. Schlögl, *Mol. Phys.*, 1992, **76**, 851; (b) X. Sun, R. Wang, B. Zhang, R. Huang, X. Huang, D. S. Su, T. Chen, C. Miao and W. Yang, *ChemCatChem*, 2014, **6**, 2270.
- Z. Zhao, Y. Dai, J. Lin and G. Wang, *Chem. Mater.*, 2014, **26**, 3151.